

# String resonances at the Large Hadron Collider

Arunava Roy\* and Marco Cavaglia†

Department of Physics and Astronomy, University of Mississippi, University, MS 38677-1848, USA

(Dated: November 1, 2018)

The Large Hadron Collider promises to discover new physics beyond the Standard Model. An exciting possibility is the formation of string resonances at the TeV scale. In this article, we show how string resonances may be detected at the LHC in the  $pp \rightarrow \gamma + jet$  channel. Our study is based on event shape variables, missing energy and momentum, maximum transverse momentum of photons and dijet invariant mass. These observables provide interesting signatures which enable us to discriminate string events from the Standard Model background.

PACS numbers: 04.60.Bc, 11.25.Wx, 04.70.Dy

## I. INTRODUCTION

Our knowledge of high energy physics is limited to energies approximately less than one TeV. A possible candidate for new physics above the TeV scale is supersymmetry (SUSY) [1, 2]. SUSY provides a solution for the Higgs mass problem, a candidate for cold dark matter, and unification of low energy gauge couplings by introducing superpartners to Standard Model (SM) fields (see Ref. [1] and references therein). Alternatives to SUSY are extra-dimensional models, such as large extra dimensions [3], warped braneworlds [4] and universal extra dimensions [5]. In these models, gravity becomes strong at the TeV scale. The most astounding consequences of TeV-scale gravity would be the production of mini black holes (BHs) [6] and real/virtual gravitons [7] in particle colliders and cosmic ray showers.

Both SUSY and extra dimensions are essential ingredients of string theory [8, 9]. The string scale is defined as [9]

$$l_s = \bar{\hbar}c\sqrt{\alpha'},$$

where  $\alpha'$  is the slope parameter with units of inverse energy squared. The strength of string interactions is controlled by the string coupling  $g_s$ . The Planck scale  $M_{PL}$  is related to the string scale  $M_s$  by

$$M_s = g_s M_{PL}.$$

Since string effects are expected to appear just before quantum gravity effects set in [10], the string coupling is generally assumed to be of order one. In this scenario, the string scale is close to the Planck scale. However, in the presence of large extra dimensions gravity becomes strong at the TeV scale. In this case the Planck scale and the string scale are both  $\sim 1$  TeV; string resonances would be observed at the Large Hadron Collider (LHC) before the onset of non-perturbative quantum gravity effects. Detection of string events at the LHC [11, 12, 13] through corrections to SM amplitudes would be the most direct evidence of this scenario.

The aim of this article is to present a detailed analysis of string resonances at the LHC in the  $pp \rightarrow \gamma + jet$  channel [11]. (For a discussion of different channels see, e.g., Ref. [12].) The main result of our investigation is that string resonances may be distinguishable from the SM background.

## II. STRING AMPLITUDE

The relevant process for  $pp \rightarrow \gamma + jet$  events is gluon-gluon scattering:  $gg \rightarrow g\gamma$ . The string amplitude for this process is [11]

$$|M(gg \rightarrow g\gamma)|^2 = g_s^4 Q^2 C(N) \left\{ \left[ \frac{s\mu(s, t, u)}{u} + \frac{s\mu(s, u, t)}{t} \right]^2 + (s \longleftrightarrow t) + (s \longleftrightarrow u) \right\}, \quad (1)$$

---

\*Electronic address: arunav@olemiss.edu

†Electronic address: cavaglia@olemiss.edu

where  $s$ ,  $t$  and  $u$  are the Mandelstam variables and

$$\mu(s, t, u) = \Gamma(1-u) \left( \frac{\Gamma(1-s)}{\Gamma(1+t)} - \frac{\Gamma(1-t)}{\Gamma(1+s)} \right). \quad (2)$$

Here  $N=3$  is the number of  $D$  branes needed to generate the eight gluons of the SM,  $C(N) = \frac{2(N^2-4)}{N(N^2-1)}$  is a constant parameter, and  $Q^2 = \frac{1}{6}\kappa^2 \cos^2 \theta_W \sim 2.55 \times 10^{-3}$ , where  $\kappa^2=0.02$  and  $\theta_W$  are the mixing parameter and the Weinberg angle, respectively. The values of the parameters are chosen as in Ref. [11].

The string amplitude possesses poles at  $n=s/M_s^2$ , where  $n$  is an integer. For odd values of  $n$  the amplitude is

$$|M(gg \rightarrow g\gamma)|^2 = g_s^4 Q^2 C(N) \frac{4}{(n!)^2} \frac{s^4 + u^4 + t^4}{M_s^4 [s - nM_s^2]} \left\{ \frac{\Gamma(t/M_s^2 + n)}{\Gamma(t/M_s^2 + 1)} \right\}^2. \quad (3)$$

For even values of  $n$  the behavior of the amplitude is obtained from Eq. (3) with the substitution  $s \rightarrow t$  and  $n \rightarrow m = t/M_s^2$  in the square bracket term. Following Ref. [11], the singularities of the amplitude are smeared with a fixed width  $\Gamma = 0.1$  for all  $n > 1$  and as

$$|M(gg \rightarrow g\gamma)|^2 \sim \frac{g_s^4 Q^2 C(N)}{M_s^4} \left\{ \frac{M_s^8}{(s - M_s^2)^2 + (\Gamma^{J=0} M_s^2)^2} + \frac{t^4 + u^4}{(s - M_s^2)^2 + (\Gamma^{J=1} M_s^2)^2} \right\} \quad (4)$$

for  $n=1$ . Equation (4) includes a correction for spin dependent widths:  $\Gamma^{J=0} = 0.75\alpha_s M_s$  and  $\Gamma^{J=1} = 0.45\alpha_s M_s$ , where  $\alpha_s = g_s^2/4\pi$  is the strong coupling constant. The presence of the poles indicates the formation of string resonances. The total cross section for the  $pp \rightarrow \gamma + jet$  event is obtained by integrating the parton cross section over the CTEQ6D parton distribution functions of the protons  $f(x, Q)$  [14]

$$\sigma_{pp \rightarrow string \rightarrow \gamma + jet} = \int_0^1 dx_1 \int_0^1 dx_2 \int_t dt f_1(x_1, Q) f_2(x_2, Q) \frac{d\sigma}{dt}, \quad (5)$$

where  $Q$  is the four-momentum transfer squared and

$$\frac{d\sigma}{dt} = \frac{|M(gg \rightarrow g\gamma)|^2}{16\pi s^2}. \quad (6)$$

The choice of CTEQ6D parton distribution functions allows direct comparison of our results to those of Ref. [11]. The

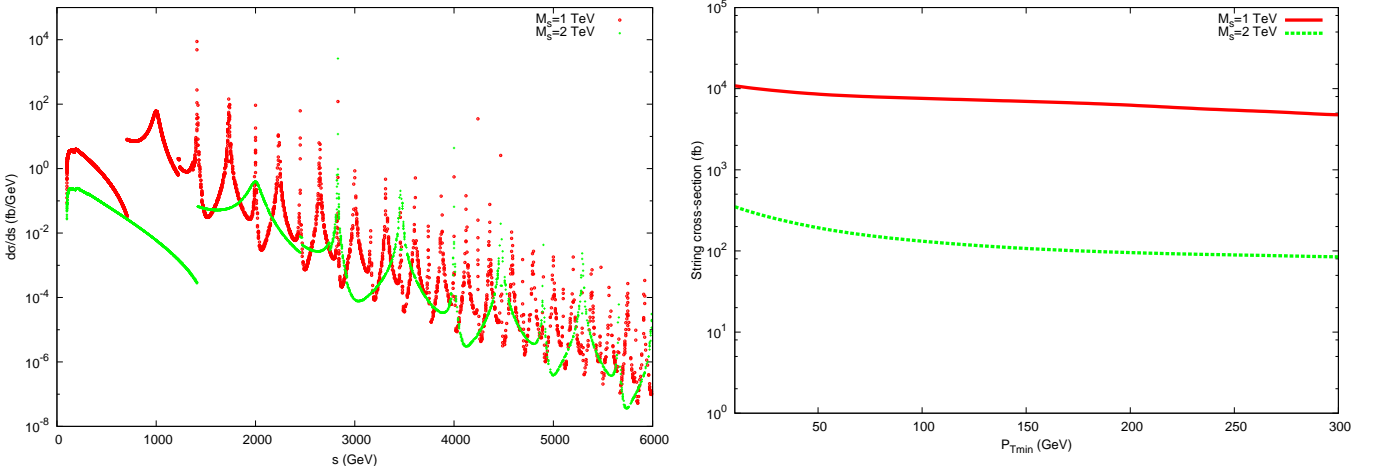


FIG. 1: Left Panel: Differential cross section of string events for  $M_s = 1$  TeV (red dots) and  $M_s = 2$  TeV (green crosses) with  $P_{Tmin}=50$  GeV. String resonances are clearly seen when  $s = nM_s^2$ . Right Panel: String cross section for  $M_s = 1$  TeV (red dots) and  $M_s = 2$  TeV (green crosses) with  $P_{Tmin}=50$  GeV. The cross section for  $M_s = 1$  TeV is  $\sim 44$  times larger than the cross section for  $M_s = 2$  TeV.

left panel of Fig. 1 shows the differential cross section of the  $pp \rightarrow \gamma + jet$  process with total center-of-mass energy  $E_{CM}$

$$\frac{d\sigma}{ds} = \int_{x_2} \int_t dx_2 dt \frac{2\sqrt{s}}{x_2 E_{CM}^2} f_1(x_1, Q) f_2(x_2, Q) \frac{d\sigma}{dt}. \quad (7)$$

The differential cross section shows resonances at  $s = nM_s^2$ . The right panel of Fig. 1 shows the total cross section as a function of the minimum transverse momenta of the two outgoing particles of the  $2 \times 2$  scattering,  $P_{Tmin}$ . The string cross section for  $M_s=1$  TeV (solid red line) and the cross section for  $M_s=2$  TeV (dashed green line) are  $\sim 5 \times 10^4$  and  $10^3$  times less than the SM cross section, respectively. Our sample run of  $10^7$  events produced  $\sim 9300$  (220) string events for  $M_s=1$  (2) TeV, with an integrated LHC luminosity of  $100 \text{ fb}^{-1}$ .

### III. ANALYSIS

String resonances at the LHC are simulated with a Fortran Monte Carlo code interfaced with PYTHIA [15]. Event-shape variables are a powerful discriminator of string events from the SM background. Their effectiveness is further increased by an analysis of events with high- $P_T$  photons. String events are characterized by high values of visible energy and missing transverse momentum as the photon and the jet originate directly from the  $2 \times 2$  interaction. Isolated photons provide a further means to extract string signals. Being directly produced from the string resonance, isolated photons from string interactions are harder than SM photons.

We fix  $P_{Tmin}=50$  GeV for both string and SM events which results into a signal-to-background ratio of  $\sim 73$ . This choice is justified as follows. For low values of  $P_{Tmin}$  the string cross section is highly suppressed *w.r.t.* the SM cross section, for example  $\frac{\sigma_{string}}{\sigma_{SM}} \sim 10^{-5}$  for  $P_{Tmin} = 10$  GeV. Therefore, discrimination of string events from the SM background is difficult for events with low  $P_{Tmin}$ . At higher values of  $P_{Tmin}$  both the SM background and the signal are substantially reduced. For example, at 300 GeV they are reduced by a factor of  $\sim 98\%$  and  $\sim 42\%$  *w.r.t.* values at  $P_{Tmin} = 50$  GeV, respectively. Thus the optimal signal-to-background ratio is obtained for  $P_{Tmin} \lesssim 100$  GeV.

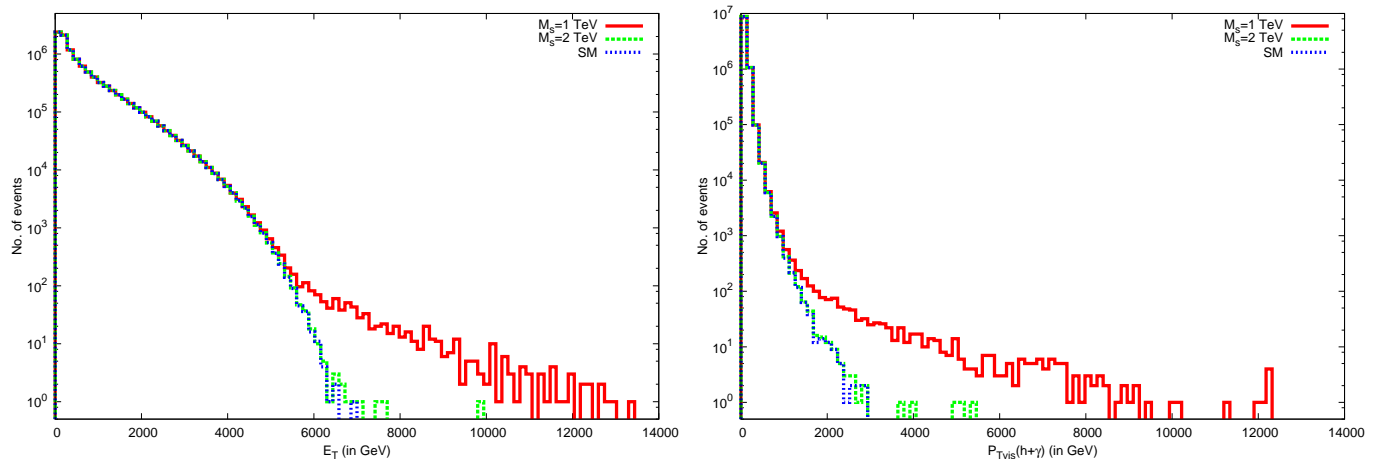


FIG. 2: Left Panel: Visible energy distribution for string+SM and SM-only events. The result for string resonances is shown by the solid red histogram ( $M_s=1$  TeV) and by the dashed green histogram ( $M_s=2$  TeV). String events can be identified from the high- $E_T$  tail for  $M_s=1$  TeV. Right Panel: Distribution of visible  $P_T$  for  $\gamma$ +hadrons. The high- $P_T$  tail is a strong indicator of the presence of string resonances.

Figure 2 shows the visible energy (left panel) and the transverse momentum of hadrons+photons (right panel) for 10 million string+SM and SM-only events. The visible energy and the transverse momentum are produced by the hard photons and the jets of the string decay. Their distributions are characterized by a long tail at high energy/momentum. The observation of events with visible energy (transverse momentum) greater than 6 (3) TeV would provide strong evidence of the formation of a string resonance.

Figure 3 shows histograms for different event shape variables. String+SM interactions generally produce a distribution of high  $P_T$  jets at slightly higher values than the SM background, i.e. string events tend to be more spherical than SM events. The jets originate from the decay of string resonances into photons and hadrons. The SM generates less heavier jets than string resonances. This is evident from the middle and right panels of Fig. 3.

In the analysis of dijets, the jets are selected according to the following criteria. The detector is assumed to have an absolute value of pseudorapidity  $\eta = -\ln\{\tan(\frac{\theta}{2})\} = 2.6$ . This ensures that the jets are originated in the hard  $2 \times 2$

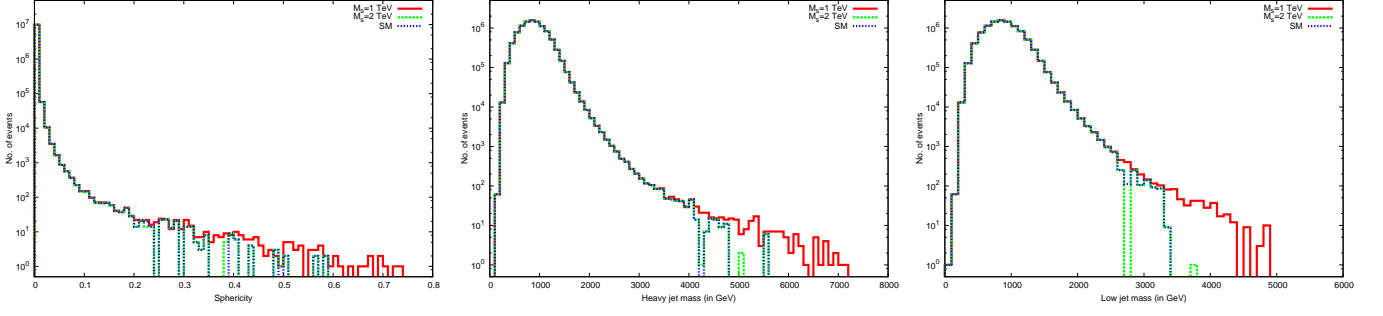


FIG. 3: Histograms of event shape variables for 10 million string+SM and SM-only events. String events are shown in solid red ( $M_s=1$  TeV) and dashed green ( $M_s=2$  TeV). SM events are shown in dotted blue. String events have on the average higher sphericity than SM events due to the slight increase in the number of jets (left panel). Similar conclusions are reached from the heavy and low jet mass distributions (middle and right panel, respectively).

scattering rather than in multiple interactions or from the beam remnants. The contribution of jets which do not originate in the hard scattering are minimized by fixing the the minimum transverse energy of all particles comprising the jet ( $\sum_i E_{T_i}$ ) to 40 GeV [16]. The particles of the jet must be within a cone of  $R = \sqrt{(\Delta\eta^2 + \Delta\phi^2)} = 0.5$  from the jet initiator, where  $\theta$  and  $\phi$  are the azimuthal and polar angles of the particle *w.r.t* the beam axis, respectively.

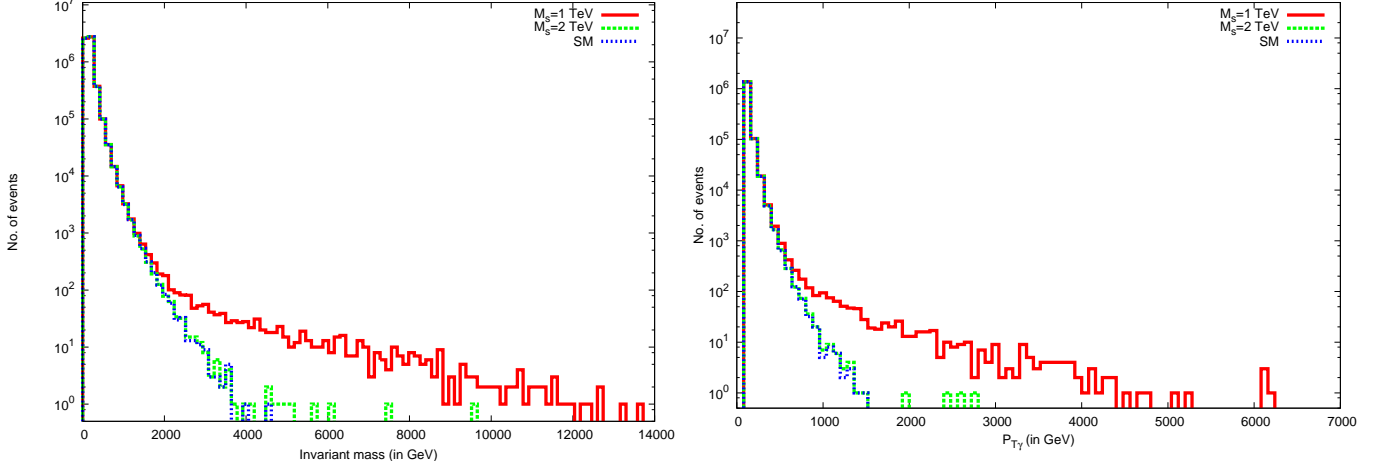


FIG. 4: Left Panel: Dijet invariant mass distribution. String decays may result in a large invariant mass. Right Panel: Distribution of the highest  $P_{T_\gamma}$  for  $1.5 \times 10^6$  events.  $\gamma$ 's with high  $P_T$  created in the string decay are the source of the long tail.

The left panel of Fig. 4 shows the invariant mass plot of the two jets with highest  $P_T$  in each event. Due to the nature of the interaction, the bulk of the events (both string+SM and SM) are comprised of dijets. These were selected using the above cuts. The jet invariant mass is

$$M_{12} = \sqrt{m_1^2 + m_2^2 + 2(E_1 E_2 - \bar{p}_1 \cdot \bar{p}_2)},$$

where  $m_{1(2)}$ ,  $E_{1(2)}$  and  $\bar{p}_{1(2)}$  are the mass, energy and momenta of jet 1 (2), respectively. As expected, the SM invariant mass distribution is negligible beyond  $\sim 4$  TeV. This is due to the production of direct soft photons and jets from the SM interaction. The string+SM distribution is characterized by a long tail up to energies of several TeV (three times more than the SM). This tail is originated from the decay of string resonances into hard jets and photons. Therefore, the measure of a large invariant mass could provide strong evidence of a string-mediated interaction.

The right panel of Fig. 4 shows the distribution of the highest  $P_{T_\gamma}$  of isolated photons for string+SM and SM-only events. Following Ref. [16], the cuts on the photon are  $P_{T_\gamma} \geq 80$  GeV,  $\eta < 2.6$  and an isolation cut  $\sum_n P_T < 7$  GeV in a cone of  $R = 0.4$ . The photons from string resonances are expected to have a higher  $P_{T_\gamma}$  than the SM photons because they are the direct products of the string decay. The main sources of background for direct photons are jet fluctuations and photons originating from the initial and final state radiation [16]. In the former case, a jet consists

of a few particles including high- $P_T$  mesons (generally  $\pi_0$  [16]). The pions decay into a pair of photons with a  $\sim 99\%$  branching ratio. Due to the high boost, the photons have a relatively small angular separation and therefore “fake” a single photon in the electromagnetic calorimeter. The rate of this process is 1 out of  $\sim 10^3$  to  $10^4$  events [16]. Other sources of fake photons are  $H \rightarrow \gamma\gamma$  [17] or processes from other exotic phenomena, e.g. SUSY [18] or large extra dimensions [3]. Isolation cuts on the photon can effectively reduce the number of fake photons.

#### IV. CONCLUSIONS

We have investigated string resonances at the LHC and shown how to differentiate them from the SM background. Our analysis has proven that string resonances could be detected when  $M_s \sim 1$  TeV. String events show higher sphericity and higher visible energy than the SM background. These quantities allow discrimination of string events from SM background when combined with the measure of the  $P_T$  of isolated photons and the dijet invariant mass. Since the final products of the string resonances are directly produced from the string decay, the dijet invariant mass is characterized by a tail at high energies which is absent in the SM.

Other exotic phenomena could also be observed at the LHC near the TeV scale, such as the formation of BHs. A powerful way of discriminating between BH and string events would be searching for a  $Z_0$  mass peak in the invariant mass of high- $P_T$  leptons.  $Z_0$  production is highly suppressed in case of string events [11]. On the contrary BH decay is characterized by the production of a variety of particles with high transverse momentum. A rough counting of the number of degrees of freedom of these particles shows that the estimated rate of hadron-to-lepton production is 5:1 and the rate of  $Z_0$  and  $\gamma$  production is comparable ( $\sim 2\%$  to  $3\%$ ) with the  $Z_0$  bosons decaying into opposite-sign leptons with a 3.4% branching ratio. Thus the invariant mass distribution of BH events peaks at  $\sim 92$  GeV, confirming the production of a  $Z_0$  boson [19]. The presence of a peak at  $\sim 92$  GeV in the invariant mass of leptons would effectively rule out formation of string resonances.

#### Acknowledgments

The authors would like to thank L. A. Anchordoqui for his many valuable suggestions and comments.

- 
- [1] S. P. Martin, arXiv:hep-ph/9709356.
  - [2] A. Bartl *et al.*, *In the Proceedings of 1996 DPF / DPB Summer Study on New Directions for High-Energy Physics (Snowmass 96)*, Snowmass, Colorado, 25 Jun - 12 Jul 1996, pp SUP112;  
H. Baer, C. h. Chen, F. Paige and X. Tata, “Signals for minimal supergravity at the CERN large hadron collider: Multi-jet plus missing energy channel,” Phys. Rev. D **52**, 2746 (1995) [arXiv:hep-ph/9503271].
  - [3] N. Arkani-Hamed, S. Dimopoulos and G. R. Dvali, Phys. Lett. B **429**, 263 (1998) [arXiv:hep-ph/9803315];  
I. Antoniadis, N. Arkani-Hamed, S. Dimopoulos and G. R. Dvali, Phys. Lett. B **436**, 257 (1998) [arXiv:hep-ph/9804398];  
N. Arkani-Hamed, S. Dimopoulos and G. R. Dvali, Phys. Rev. D **59**, 086004 (1999) [arXiv:hep-ph/9807344].
  - [4] L. Randall and R. Sundrum, Phys. Rev. Lett. **83**, 3370 (1999) [arXiv:hep-ph/9905221].
  - [5] T. Appelquist, H. C. Cheng and B. A. Dobrescu, Phys. Rev. D **64**, 035002 (2001) [arXiv:hep-ph/0012100].
  - [6] P. C. Argyres, S. Dimopoulos and J. March-Russell, Phys. Lett. B **441**, 96 (1998) [arXiv:hep-th/9808138];  
T. Banks and W. Fischler, arXiv:hep-th/9906038;  
S. Dimopoulos and G. Landsberg, Phys. Rev. Lett. **87**, 161602 (2001) [arXiv:hep-ph/0106295];  
S. B. Giddings and S. D. Thomas, Phys. Rev. D **65**, 056010 (2002) [arXiv:hep-ph/0106219];  
E. J. Ahn, M. Cavaglià and A. V. Olinto, Phys. Lett. B **551**, 1 (2003) [arXiv:hep-th/0201042];  
V. P. Frolov and D. Stojkovic, Phys. Rev. Lett. **89**, 151302 (2002) [arXiv:hep-th/0208102];  
M. Cavaglià, S. Das and R. Maartens, Class. Quant. Grav. **20**, L205 (2003) [arXiv:hep-ph/0305223];  
A. Chamblin, F. Cooper and G. C. Nayak, Phys. Rev. D **70**, 075018 (2004) [arXiv:hep-ph/0405054];  
B. Koch, M. Bleicher and H. Stoecker, J. Phys. G **34**, S535 (2007) [arXiv:hep-ph/0702187];  
D. M. Gingrich, JHEP **0711**, 064 (2007) [arXiv:0706.0623 [hep-ph]];
  - J. L. Feng and A. D. Shapere, Phys. Rev. Lett. **88**, 021303 (2002) [arXiv:hep-ph/0109106];  
L. A. Anchordoqui, J. L. Feng, H. Goldberg and A. D. Shapere, Phys. Rev. D **65**, 124027 (2002) [arXiv:hep-ph/0112247];  
E. J. Ahn, M. Ave, M. Cavaglià and A. V. Olinto, Phys. Rev. D **68**, 043004 (2003) [arXiv:hep-ph/0306008];  
J. I. Illana, M. Masip and D. Meloni, Phys. Rev. D **72**, 024003 (2005) [arXiv:hep-ph/0504234];

- E. J. Ahn and M. Cavaglià, Phys. Rev. D **73**, 042002 (2006) [arXiv:hep-ph/0511159];  
M. Cavaglià and A. Roy, Phys. Rev. D **76**, 044005 (2007) [arXiv:0707.0274 [hep-ph]];  
M. Cavaglià, Int. J. Mod. Phys. A **18**, 1843 (2003) [arXiv:hep-ph/0210296];  
R. Emparan, *Black hole production at a TeV*, arXiv:hep-ph/0302226;  
S. Hossenfelder, *What black holes can teach us*, arXiv:hep-ph/0412265;  
P. Kanti, Int. J. Mod. Phys. A **19**, 4899 (2004) [arXiv:hep-ph/0402168];  
G. Landsberg, J. Phys. G **32**, R337 (2006) [arXiv:hep-ph/0607297].
- [7] G. F. Giudice, R. Rattazzi and J. D. Wells, Nucl. Phys. B **544**, 3 (1999) [arXiv:hep-ph/9811291];  
E. A. Mirabelli, M. Perelstein and M. E. Peskin, Phys. Rev. Lett. **82**, 2236 (1999) [arXiv:hep-ph/9811337];  
S. Cullen and M. Perelstein, Phys. Rev. Lett. **83**, 268 (1999) [arXiv:hep-ph/9903422].
- [8] J. Polchinski, “String theory. Vol. 1 & 2” *Cambridge, UK: Univ. Pr. (1998)*
- [9] B. Zwiebach, “A first course in string theory,” *Cambridge, UK: Univ. Pr. (2004)*
- [10] K. R. Dienes, Phys. Rept. **287**, 447 (1997) [arXiv:hep-th/9602045].
- [11] L. A. Anchordoqui, H. Goldberg, S. Nawata and T. R. Taylor, Phys. Rev. D **78**, 016005 (2008) [arXiv:0804.2013 [hep-ph]].
- [12] P. Burikham, T. Figy and T. Han, Phys. Rev. D **71**, 016005 (2005) [Erratum-ibid. D **71**, 019905 (2005)] [arXiv:hep-ph/0411094].
- [13] L. A. Anchordoqui, H. Goldberg, D. Lust, S. Nawata, S. Stieberger and T. R. Taylor, arXiv:0808.0497 [hep-ph].
- [14] J. Pumplin, D. R. Stump, J. Huston, H. L. Lai, P. M. Nadolsky and W. K. Tung, JHEP **0207**, 012 (2002) [arXiv:hep-ph/0201195].
- [15] T. Sjostrand, S. Mrenna and P. Skands, JHEP **0605**, 026 (2006) [arXiv:hep-ph/0603175];  
<http://www.thep.lu.se/~torbjorn/Pythia.html>.
- [16] P. Gupta, B. C. Choudhary, S. Chatterji, S. Bhattacharya and R. K. Shivpuri, arXiv:0705.2740 [hep-ex].
- [17] M. Pieri, S. Bhattacharya, I. Fisk, J. Letts, V. Litvin and J. G. Branson, CERN-CMS-NOTE-2006-112.
- [18] A. Abulencia *et al.* [CDF Collaboration], Phys. Rev. Lett. **99**, 121801 (2007) [arXiv:0704.0760 [hep-ex]].
- [19] A. Roy and M. Cavaglià, Phys. Rev. D **77**, 064029 (2008) [arXiv:0801.3281 [hep-ph]];  
A. Roy and M. Cavaglià, Mod. Phys. Lett. A **23**, 2987 (2008) [arXiv:0710.5490 [hep-ph]].